Astronomy
&
Astrophysics

On the origin of the X-ray emission towards the early Herbig Be star MWC 297

Jorick S. Vink[1], P. M. O'Neill[1], S. G. Els[2], and J. E. Drew[1]

[1] Imperial College London, Blackett Laboratory, Prince Consort Road, London, SW7 2AZ, UK
e-mail: jsv@astro.keele.ac.uk
[2] California Institute of Technology, Mail Code 102-8, 1200 E. California Blvd., Pasadena CA 91125, USA

Abstract. We present high resolution ($\simeq 0.2''$) AO-corrected coronographic near-infrared imaging on the early-type Herbig Be star MWC 297. X-ray flaring has been reported towards this young object, however this has been difficult to reconcile with its early spectral type (B1.5) and relatively high mass ($\sim 10\ M_\odot$). Our infrared and X-ray analysis shows that the X-ray flaring is likely due to a late-type star in the same field. The case of MWC 297 emphasizes the need for coronographic imaging to address the reality of X-ray emission towards Herbig Ae/Be stars, which is needed to understand the differences between low and high-mass star formation.

Key words. stars: formation – stars: pre-main sequence – stars: flare – stars: individual: M 297 – X-rays: stars

1. Introduction

Herbig Ae/Be stars are pivotal young stellar objects for understanding the physical differences between low and high mass star formation, as their masses ($\simeq 2$–$15\ M_\odot$) make them transitional between the low-mass T Tauri and massive stars.

X-ray emission is frequently seen in early-type O stars, where the X-ray emission arises from shocks in radiatively-driven winds (Lucy & White 1980), but the X-ray emission ceases for B stars. On the cool side of the Hertzsprung-Russell Diagram (HRD), late-type stars are magnetically active due to the presence of convective outer layers (at ~G and later types). In between these two extremes, B and A stars are not considered to be magnetically active (except Am stars), and are generally X-ray quiet.

A different story might hold for the pre-main sequence (PMS) Herbig Ae/Be stars. Zinnecker & Preibisch (1994) and Damiani et al. (1994) found that 30–50% of the Herbig stars surveyed with the ROSAT and EINSTEIN satellites emit copious amounts of X-rays. Although A stars do not have convective outer layers, there may be magnetic activity due to a seed magnetic field. In fact, the magnetic accretor model – generally applied to lower mass PMS T Tauri stars – may also be at work in Herbig Ae stars (Vink et al. 2002; Hubrig et al. 2004). This might be consistent with the X-ray flaring seen in some Herbig Ae stars (e.g. Giardino et al. 2004), but whether this scenario may hold for earlier type objects is questionable given the different circumstellar properties of the Herbig Ae and Be stars (Vink et al. 2002; Eisner et al. 2003). It is

therefore surprising that X-ray flaring has been discovered in the massive Herbig Be star MWC 297 with the ASCA X-ray satellite (Hamaguchi et al. 2000, 2005). As MWC 297 has a spectral type as early as B1.5 (Drew et al. 1997), this represents a significant puzzle to early stellar evolution theory for intermediate-mass ($\sim 10\ M_\odot$) B stars, and raises the question whether new physical effects in this part of the HRD need to be identified.

In surveys of Herbig X-ray emission (Zinnecker & Preibisch 1994; Damiani et al. 1994), X-ray luminosities (L_X) were found to be correlated with bolometric luminosity (L_{bol}): as a result the X-rays were attributed to wind shocks – similar to the O star mechanism. But Herbig Ae/Be winds are probably not fast enough for radiatively-driven wind shocks to develop. At the same time, the option of unresolved companions was considered unlikely in view of the L_X versus L_{bol} relationship. However, Testi et al. (1998) have found that the number of late-type companions to Herbig Ae/Be stars grows with increasing mass and L_{bol}. This re-opens the possibility that at least some of the X-ray emission towards Herbig stars is due to one or more late-type companions.

In this paper, we address the question of whether the X-ray flaring of MWC 297 originates from MWC 297 itself or from a late-type companion. Although many sources around Herbig Ae/Be stars have been imaged at separations of 100–10 000 AU (Li et al. 1994; Pirzkal et al. 1997; Leinert et al. 1997; Smith et al. 2005), companions around the more luminous objects are much more challenging to discover. Most imaging studies of Herbig stars identify objects at relatively large distances

($\simeq 10\,000$–$100\,000$ AU) from the central object (e.g. Testi et al. 1998). The fact that no sources have been detected close to MWC 297, does not mean that they are not there, especially since MWC 297, with an H-band magnitude of 4.4, may completely outshine any close-in companions.

Progress may be made through Adaptive Optics (AO) coronographic imaging – a technique that has only recently become available. At X-ray wavelengths, early studies with satellites such as ROSAT, EINSTEIN, and ASCA were generally subject to relatively poor spatial resolution, but the CHANDRA satellite offers spatial resolution of the order of $1''$. CHANDRA might well be capable of resolving many putative low-mass companions, as exemplified by the study of

Stelzer et al. (2003) on late-type B stars. Here we report combined infrared AO-coronographic imaging with high resolution X-ray imaging of the extreme case of MWC 297.

2. Observations

2.1. Coronographic Adaptive Optics

The AO-corrected H-band imaging data were obtained during the night of 2004 July 31 with the Optimised Stellar Coronograph OSCA (Thompson et al. 2003). included in the NAOMI AO system (Myers et al. 2003) on the 4.2-m William Herschel Telescope (WHT), La Palma. We used an occulting mask of $1.0''$ to block the light of the central object. Using this mask, it is possible to suppress the bright core of the stellar point-spread function (PSF) and lower its wings by $\Delta H \sim$ 6.5 mag for distances from the central star of $\sim 1''$. The NAOMI PSF also includes the diffraction pattern of the segmented deformable mirror (DM). We took sets of observations under various position angles (PAs of 0, 30, 60 and 120 degrees), as the diffraction pattern remains constant over the chip this allows us to also inspect areas that would otherwise remain hidden in the diffraction pattern. We obtained 2×10 sets of 20 co-averaged images with an exposure time of 1 s for each PA. In addition, we imaged stars with no known companions as PSF references after each PA set. The atmospheric conditions were good and the AO corrected images yield a $FWHM$ of $\sim 0''.2$. The centring of the mask over the star was done manually. Basic data reduction included dark, and flatfield subtraction as well as bad pixel removal, which was performed using the ESO software packages `eclipse` and MIDAS.

2.2. X-ray observations with CHANDRA and ASCA

CHANDRA observed MWC 297 in a single visit (observation ID 1883) on 2001 September 21 and 22, for ~ 11 hours, using the default ACIS-I chips (I0-I3, S2, S3). An aspect correction[1] was applied to the level 1 events file, such that the 90% confidence error circle has a radius of $0.6''$. New level 2 events files were created in the standard manner using CIAO 3.2.1 and CALDB 3.0.1. The resulting good exposure time was ~ 37 ks. A 0.3–10 keV image was extracted and source detection was performed using the CIAO tool `wavdetect`. Source counts were
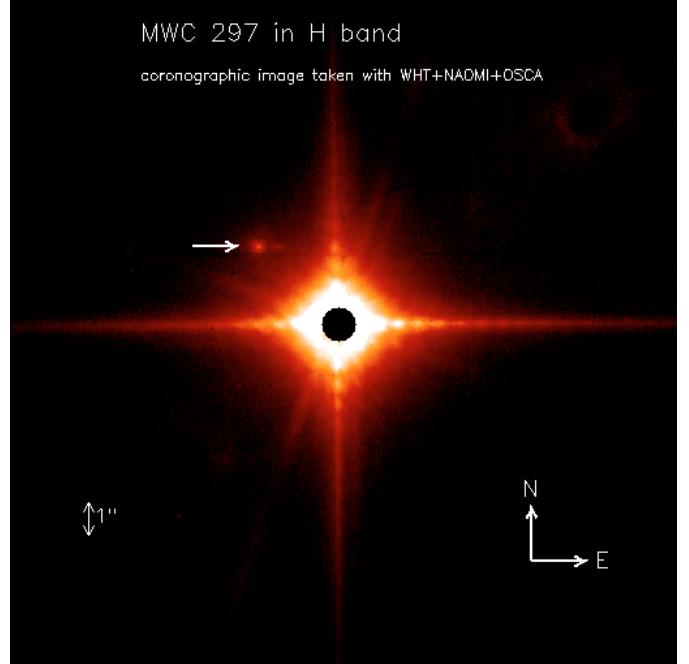

Fig. 1. OSCA H-band image of MWC 297. The logarithmically-scaled image shows the presence of a faint source close to the bright star, at PA = 313°. In order to increase the visibility of this object we placed a numerical mask over the central region which is covered by the instrumental coronographic mask.

extracted using a circular region centred on each source, with a radius of either 3 or 5 pixels (see Sect. 3.2). Background counts were extracted from an annulus with a width of 100 pixels centred on the source aperture. The inner radius of the annulus was set to be twice the source region radius. An exposure map was generated, and this was used to determine the scaling factor between the source and background regions. The estimated mean number of background counts in each of the source regions is ~ 0.4 counts.

ASCA observed MWC 297 three times (with sequence numbers 21007000, 21007010, 21007020) between 1994 April 8 and 12. These data were presented previously by Hamaguchi et al. (2000, 2005). Here we only discuss the ~ 6 h observing sequence 21007010, during which the decay phase of an X-ray flare was observed. Moreover, we restricted our analysis to the data from the two Solid-state Imaging Spectrometers (SIS), SIS0 and SIS1, as these instruments have higher spatial resolution than the Gas Imaging Spectrometers on ASCA. The PSF of the SIS instruments have a core with a $FWHM$ of $\sim 50''$ (Jalota et al. 1993). The data were screened using the Tartarus[2] analysis pipeline, which yielded a good exposure time of ~ 4.7 ks for each SIS instrument. Sky images in the 0.5–10 keV band were extracted for each SIS using a spatial binning of $1.6''$ per spixel. These images were then combined and smoothed with a Gaussian kernel having a $FWHM$ of 4 pixels. The source position calibration of the "REV2" data in the ASCA archive has a 90% confidence error circle with radius

---

[1] http://cxc.harvard.edu/cal/ASPECT/fix_offset/
fix_offset.cgi

[2] http://astro.imperial.ac.uk/Research/Tartarus/
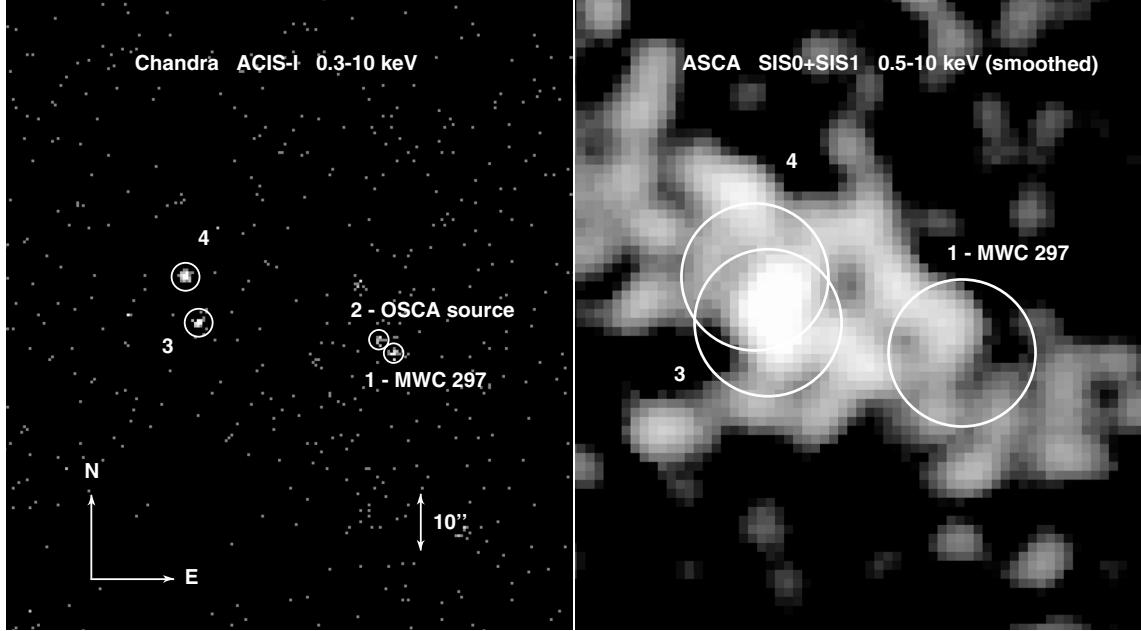
Fig. 2. CHANDRA (*left*) and ASCA (*right*) images of the MWC 297 field. Note the presence of two X-ray sources in the CHANDRA image, with a separation of $\simeq 3.5''$ at PA of $\simeq 315^{\circ}$. The ASCA image (same scale) is from the observation during which the source was seen to flare, and clearly shows the much larger PSF of ASCA. The positions of the CHANDRA sources 1 (MWC 297), 3, and 4 are shown, along with the error circles. Note that, in the ASCA image, the observed peak in intensity is consistent with positions of sources 3 and 4, but not with that of MWC 297.

$\sim 40''$ (Gotthelf 1996). A later calibration allows this pointing accuracy to be improved, with the 90% confidence error being reduced to a radius of $12''$. We used the on-line look-up table[3] to restore the astrometric accuracy of our combined SIS0+SIS1 image.

3. Results

3.1. Coronographic Adaptive Optics

Figure 1 shows the OSCA H-band image of MWC 297. We report the discovery of a faint object located $3.39'' \pm 0.2''$ along position angle (PA) $313^{\circ} \pm 2^{\circ}$ (northwest) from MWC 297. Given the fact that the newly found source rotates with the rotator position, we consider the detection to be real. Some other features are visible, in particular a large cross-like pattern extending over almost the entire field and two fainter spikes at PAs of $\sim 70^{\circ}$ and 250°. The cross-like feature is the DM's diffraction pattern, whereas the latter is due to the secondary spider. Finally, a small fainter structure can be seen just east of the newly detected source. As its position does not change on the sky in accordance with the rotator angle, this structure is considered to be an instrumental artifact.

Although we have not proven a physical relationship between MWC 297 and the newly discovered object, the projected separation of 850 AU (distance to MWC 297 = 250 pc; Drew et al. 1997) is consistent with the new source being a binary companion or to have formed from the same cloud core as MWC 297 (Li et al. 1994).

---

[3] `http://heasarc.gsfc.nasa.gov/docs/asca/coord/update.html`

Accurate photometry of the newly found object is challenging as it is found close to the bright host star. Using the 2MASS H-band magnitude of MWC 297, we calibrated our zeropoint by using open-loop images of MWC 297. PSF photometry on the companion was performed by fitting Gaussians. In addition, we performed aperture photometry. The resulting H-band magnitudes agree fairly well with each other, and we find an H-band magnitude difference of $\Delta H = 8.5 \pm 0.25$ mag. Using the 2MASS magnitude of MWC 297, we find $H = 12.9 \pm 0.25$ mag for the OSCA source. To investigate whether our discovered object at a PA of 313° could be responsible for the X-ray flaring of MWC 297, we turn to the relevant archival X-ray satellite data.

3.2. CHANDRA and ASCA results

The CHANDRA X-ray image of the region near MWC 297 is shown in the left panel of Fig. 2, where we note four objects. The positions of these objects are listed in Table 1. The two X-ray sources with a separation of $\simeq 3.5''$ at PA of $\simeq 315^{\circ}$ are an exact match to our H-band imaging of MWC 297 (source 1) and our newly discovered source (source 2). Note that if source 1 and 2 form a binary system, the large period – implied by the 850 AU separation – means that proper motion will not be significant, and source 2 will be at the same position in the OSCA and CHANDRA images. We cannot exclude the possibility that the remaining X-ray emission from source 1, which is consistent with MWC 297's position, is yet due to one or more other companions that remain unresolved in the OSCA image. Also visible in the CHANDRA image are sources 3 and 4, at roughly $35''$ from MWC 297. Source counts were extracted using a radius of 3 pixels for sources 1 and 2, and a radius

Table 1. The four sources seen in the CHANDRA field.

#	Name	RA	Dec	counts	H
1	MWC 297	18 27 39.54	−03 49 52.0	23	4.4[1]
2	OSCA source	18 27 39.36	−03 49 49.6	13	12.9[2]
3	2MASS J18273723-0349466	18 27 37.24	−03 49 46.7	58	11.3[1]
4	2MASS J18273709-0349385	18 27 37.09	−03 49 38.6	61	9.4[1]

[1] 2MASS [2] WHT/OSCA (this paper).

of 5 pixels for sources 3 and 4. The total 0.3–10 keV source counts are listed in Table 1. Note that the sum of source counts from sources 3 and 4 is about three times greater than that for sources 1 and 2. These CHANDRA data raise the question of whether the low spatial resolution of ASCA may have led to a misidentification of the reported X-ray flaring of MWC 297. We therefore turn to the ASCA flaring data.

Figure 2 (right) shows the combined SIS image of the ASCA flaring data on MWC 297 – on the same scale as the CHANDRA image. We have indicated the positions of CHANDRA sources 1, 3, and 4. The circles in this image have radii of 13″, indicating the combined ASCA and CHANDRA position uncertainty. It is immediately apparent from Fig. 2 (right) that the CHANDRA sources are confused in the ASCA image. Moreover, the improved astrometry provided by the corrections of Gotthelf et al. (2000) shows that the peak of the observed emission in the ASCA PSF is inconsistent with the position of sources 1 and 2. Instead, the peak is consistent with the positions of source 3 or 4. This strongly suggests that the origin of the flaring behaviour is due to source 3 or 4. Their positions line up with 2MASS point sources, with H = 11.3 and 9.4 for sources 3 and 4 respectively. Given the fact that source 4 has a larger $(H-K)$ IR excess than source 3, the X-ray flaring is most likely due to source 4. In any case, at the distance of MWC 297, these H-band magnitudes are consistent with a T Tauri nature.

4. Conclusions

We have presented high resolution AO-NIR and X-ray imaging on MWC 297. Given the early spectral type of the object (B1.5), the reported X-ray flaring of this early Herbig Be star has been difficult to understand. Using CHANDRA, we have resolved the X-ray emission from objects surrounding MWC 297 and found that the brightest X-ray source is not associated with MWC 297 itself. Furthermore, we have shown that the peak of the observed ASCA flaring is inconsistent with the position of MWC 297. Instead, it is most likely due to a late-type source in the Herbig Be star's field.

The study by Stelzer et al. (2003) on late-type B stars, as well as our coronographic study of the young massive object MWC 297 presented here emphasize the need for high spatial resolution X-ray and infrared imaging to verify the origin of X-ray emission attributed to Herbig Ae/Be stars. This will assist in a proper evaluation of the physical differences governing low and high-mass star formation.

References

Damiani, F., Micela, G., Sciortino, S., & Harnden, F. R. Jr. 1994, ApJ, 436, 807

Drew, J. E., Busfield, G., Hoare, M. G., et al. 1997, MNRAS, 286, 538

Giardino, G., Favata, F., Micela, G., & Reale, F. 2004, A&A, 413, 669

Gotthelf, E. 1996, ASCA News, 4, 31

Gotthelf, E. V., Ueda, Y., Fujimoto, R., Kii, T., & Yamaoka, K. 2000, ApJ, 543, 417

Hamaguchi, K., Terada, H., Bamba, A., & Koyama, K. 2000, ApJ, 532, 1111

Hamaguchi, K., Yamauchi, S., & Koyama, K. 2005, ApJ, 618, 360

Hubrig, S., Schöller, M., & Yudin, R. V. 2004, A&A, 428, 1

Jalota, L., Gotthelf, E. V., & Zoonematkermani, S. 1993, Proc. SPIE, 1945, 453

Leinert, C., Richichi, A., & Haas, M. 1997, A&A, 318, 472

Li, W., Evans, N. J., Harvey, P. M., & Colome, C. 1994, ApJ, 433, 199

Lucy, L. B., & White, R. L. 1980, ApJ, 241, 300

Myers, R. M., et al. 2003, Proc. SPIE, 4839, 67

Pirzkal, N., Spillar, E. J., & Dyck, H. M. 1997, ApJ, 481, 392

Smith, K. W., Balega, Y. Y., Duschl, W. J., et al. 2005, A&A, 431, 307

Stelzer, B., Huélamo, N., Hubrig, S., Zinnecker, H., & Micela, G. 2003, A&A, 411, 517

Testi, L., Palla, F., & Natta, A. 1998, A&AS, 133, 81

Thompson, S., Doel, A. P., Bingham, R. G., et al. 2003, Proc. SPIE, 4839, 1085

Vink, J. S., Drew, J. E., Harries, T. J., & Oudmaijer, R. D. 2002, MNRAS, 337, 356

Zinnecker, H., & Preibisch, Th. 1994, A&A, 292, 152